Concomitant Intercalation and Decomplexation of Ferrocene Sulfonates in Layered Double Hydroxides

Sandrine Morlat-Thérias,* Christine Mousty,* Pierre Palvadeau,†,[1] Philippe Molinié,†
Philippe Léone,† Jean Rouxel,† Christine Taviot-Guého,‡ Abderrahman Ennaqui,‡
André de Roy,‡ and Jean Pierre Besse‡

*SEESIB UMR CNRS 6504, 63177 Aubiere cedex, France; †IMN chimie des solides, UMR CNRS 6502, BP 32229, 44322 Nantes cedex 3, France; and ‡LMI, UPRES A 6002, 63177 Aubiere cedex, France

In the [Zn–Cr–Cl] lamellar double hydroxide corresponding to the chemical formula $[Zn_2^{2+}Cr^{3+}(OH^-)_6]$ $[Cl^-, 2H_2O]$, chlorine anions can be easily exchanged by various moieties. For example, it is possible to replace Cl^- ions with ferrocene mono- and disulfonate salts in the interlamellar space. In a second step, these organic molecules can be removed by carbonate ions. XPS, EXAFS, Mössbauer spectroscopy, and magnetic measurements show that during this last exchange ferrocene sulfonates are decomplexed, liberating Fe^{3+} ions which then would be introduced into the hydroxide layers. The main consequence is a modification of magnetic properties. © 1999 Academic Press

INTRODUCTION

The anion exchange properties of layered double hydroxides (LDH) are well known (1–4). These layered materials are able to intercalate neutral guest molecules or to exchange inorganic and organic ions. In particular, a very large range of organic guests may be incorporated into LDH creating an inorganic–organic supramolecular structure with various potential applications (4). Particularly, we have previously realized a structural and electrochemical characterization of LDH exchanged with anions bearing one or two sulfonate groups (5–8). This paper deals with the characterization of intercalated ferrocene derivatives (mono- and disulfonate salts, written FMS and FDS). The electrochemical behavior of these redox anions intercalated into LDH interlayers has been published elsewhere (9). The reversibility of the oxidation process within these hybrid materials has been studied by cyclic voltammetry, showing the role of the electrolyte anions. An electrochemical transfer at LDH modified electrodes via an intercrystalline mechanism was confirmed.

In this paper, we report the modifications of structural and physical properties induced by these intercalations. Layered double hydroxides contain positively charged brucite type layer and exchangeable anions in the interlamellar space together with water molecules. They are represented by the general formula $[M_n^{2+}M'^{3+}(OH^-)_{2n+2}]$ $[X^-, 2H_2O]$ in which $M = Zn^{2+}$, Co^{2+}, Mg^{2+}, Ca^{2+}..., $M' = Cr^{3+}$, Al^{3+}, Fe^{3+}..., $X = Cl^-$, CO_3^{2-}, SO_4^{2-}... for example (2), and abbreviated hereafter as $[M–M'X]$. The starting LDH used here is [Zn–Cr–Cl]. The [Co–Fe–Cl] double hydroxide is our reference for physical characterizations. In [Zn–Cr–FMS] and [Zn–Cr–FDS] compounds, a complete intercalation of ferrocene sulfonates would lead to a ratio FMS/Cr or FDS/Cr of 1 and 0.5, respectively.

EXPERIMENTAL

Sodium or ammonium salts of monosulfonic FMS and disulfonic FDS ferrocenes were obtained by direct sulfonation of ferrocene with chlorosulfonic acid (9, 10). LDH [Zn–Cr–FMS] and [Zn–Cr–FDS] were prepared by a classical coprecipitation. We used 5.4 ml of an aqueous solution containing zinc chloride (1.44×10^{-3} mol) and chromium chloride (7.2×10^{-4} mol) was added dropwise to a stirred solution (20 ml) of decarbonated water containing two equivalents in charge of organic anions (FcMS or FcDS) per mol of chromium over a period of 36 h. The solution was maintained under nitrogen atmosphere in order to minimize the contamination with atmospheric CO_2. A solution of sodium hydroxide (1 M) was simultaneously added by means of a pH regulator via a pH electrode immersed in the reagent solution in order to fix the pH of coprecipitation at 5.0. The precipitates were separated by centrifugation, washed with deionized water, and dried at room temperature. The reverse anion exchange reactions were performed with 5 M Na_2CO_3 solution leading to [Zn–Cr–FMS/CO_3] and [Zn–Cr–FDS/CO_3].

The composition of the samples was checked by elemental analyses (Service Central d'analyse of the CNRS at Vernaison) and EDX analyses were made with a JEOL 5800LV electron microscope equipped with a PGT IMIX system. EDX technique was mainly used to determine the ratio between metallic atoms, i.e., Fe/Cr or Fe/Zn. Powder X-ray diffraction data were collected with a Siemens D500 diffractometer using a radiation source $CuK\alpha = 1.5418$ Å. Mössbauer spectra of the samples were obtained by using a constant acceleration automatic folding Elscint-type spectrometer with a room temperature ^{57}Co source in a transmission geometry. The data were computed with a least-squares fitting procedure with Lorentzian lines. Fe_α was used as a standard reference. Magnetic measurements were performed in the 5–300 K temperature range with a MPMS Quantum Design magnetometer. X-ray absorption data were recorded at the Fe–K edge in transmission geometry on the EXAFS IV beamline at the high-energy synchrotron ring of the Laboratoire pour l'Utilisation du Rayonnement Electromagnetique (LURE, Orsay France). The finely powered samples were embedded in spectroscopic grade boric acid and pressed into discs. The EXAFS analyses were carried out using programs written by A. Michalowicz (11). Finally, the XPS measurements were performed on a Scienta ESCA 300, (Al$K\alpha$) at Lise, Université Notre-Dame de la Paix in Namur by J. Riga using a high-power rotating anode (4100 rpm) and the monochromatized Al$K\alpha$ radiation (1486.6 eV).

RESULTS AND DISCUSSION

The layered structure of the intercalated compounds was checked by X-Ray powder diffraction data (PXRD). The PXRD patterns for all samples are presented in Fig. 1. Lattice parameters c ($d = c/3$) and a have been calculated from spacings due to planes (00l) and (110), respectively, assuming a rhombohedral symmetry $R\bar{3}m$. The gallery height d increases from 7.7 Å in a pure [Zn–Cr–Cl] to 15.0 Å in [Zn–Cr–FDS] and 20.0 Å in [Zn–Cr–FMS]. The presence of organic anions expands the interlayer space of the LDH to basal spacings between depending on the size of the guest molecules calculated with molecular models (Alchemy software) and their arrangement in the internal galleries. The quality of spectra decreases with intercalation and after the inverse exchange, only few diffraction lines are observed.

Ferrocene has an aproximatively cubic shape of about 4.1 Å (12), the total anion size including $-SO_3^-$ bonding length is 6.0 Å for FMS and 7.5 Å for FDS. The d spacing of [Zn–Cr–FcDS] ($d = 15.0$ Å) suggests that the metal-ring centroid axes of the ferrocene guest anions are oriented parallel to the host layers as reported for various organometallic sandwich complexes in transition metal oxyhalides (13) or lamellar dichalcogenides (14) (Fig. 2a).
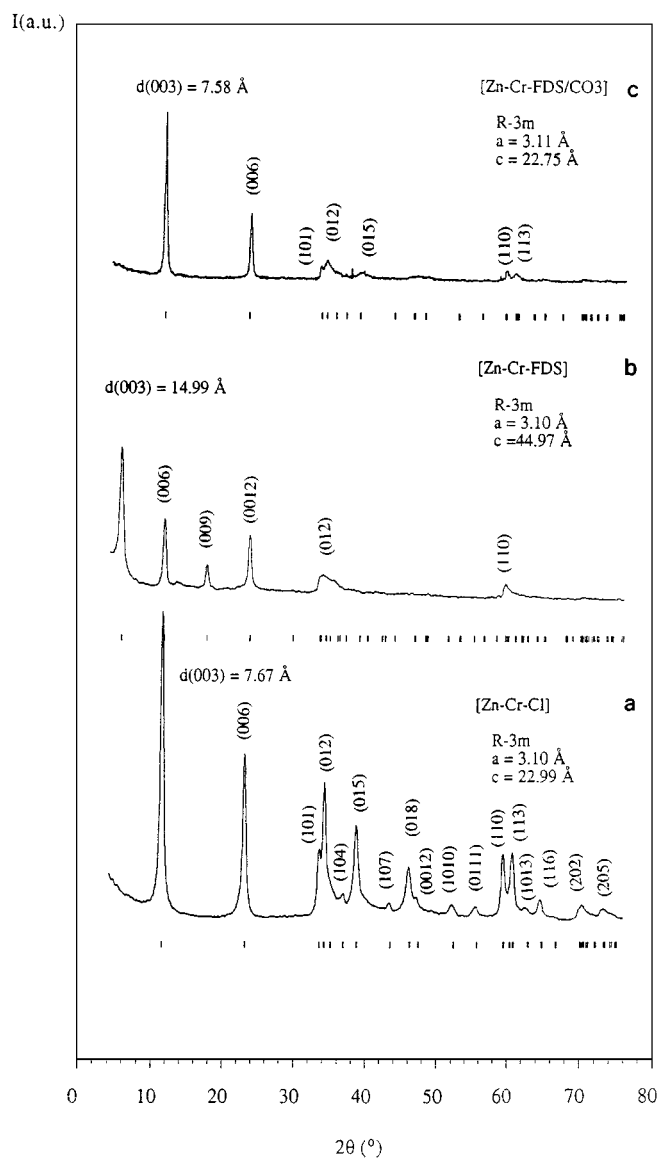

FIG. 1. Powder X-Ray diffraction patterns of (a) [Zn–Cr–Cl], (b) [Zn–Cr–FDS], and (c) [Zn–Cr–FDS/CO$_3$].

Taking into account the thickness of the brucite layers ca. 2.1 Å and strong hydrogen bonds ($d_{O-H-O} = 2.7$ Å) as observed with other disulfonate organic anions intercalated in LDH interlayer spaces [8], this involves an overall basal spacing $d_{calc} = l_{lay} + 2 l_{O-H-O} + l_{an} = 2.1 + 2 (2.7 \pm 0.1) + 7.5 = 15$ Å corresponding to the experimental data.

On the other hand, it is noteworthy that the d spacings are systematically higher with monosulfonate than disulfonate anions ($\delta \cong 5$ Å) (8) as in the case of acetylferrrocene intercalated in the MoS$_2$ lattice (15). Indeed, in this case, the calculated basal spacing would be $d_{calc} = 2.1 + 2 (2.7 \pm 0.1) + 2 \times 6 = 19.5$ Å close to the experimental value 20.0 Å assuming the formation of a bilayer of FMS (Fig. 2b).
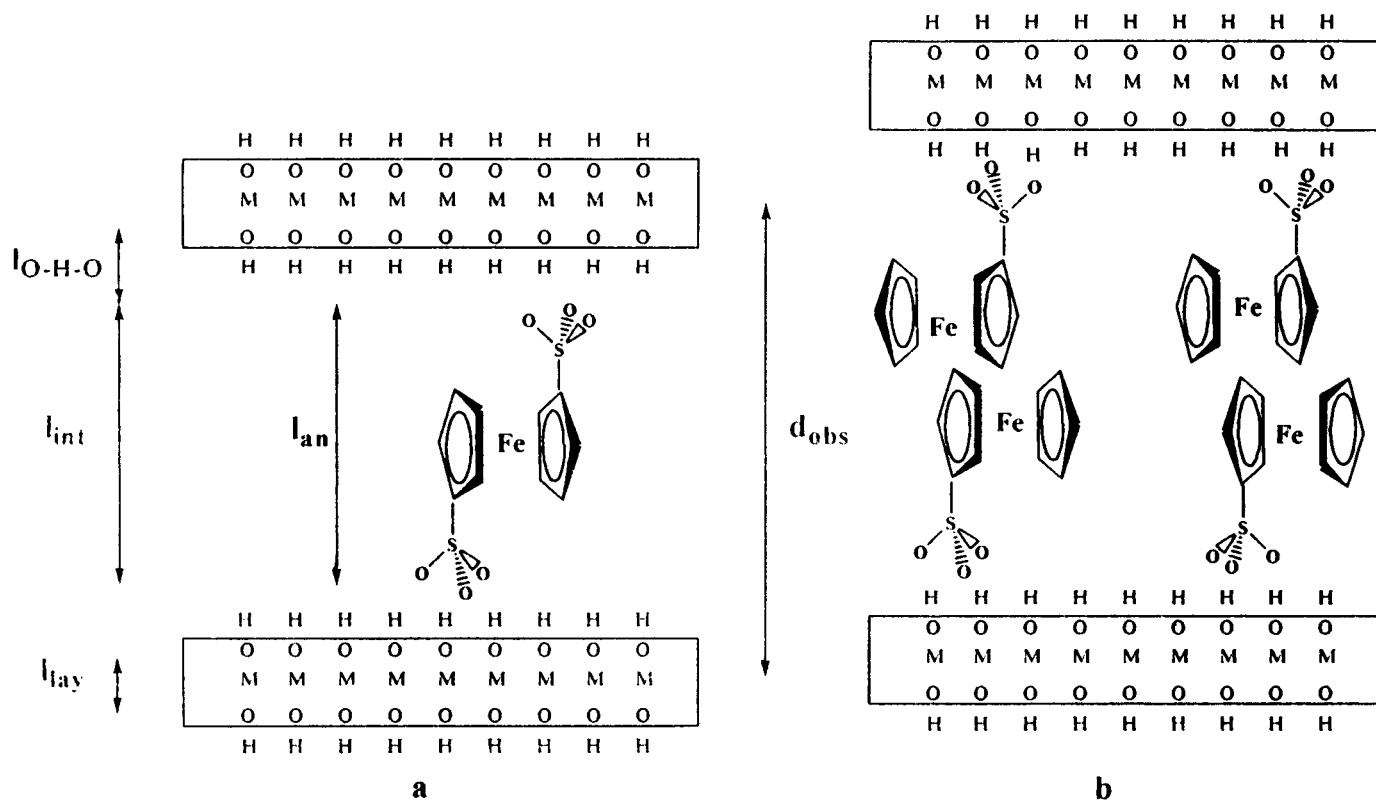
FIG. 2. Schematic representation of the intercalation of ferrocene sulfonates in LDH: (a) single layer of ferrocene bisulfonate, (b) double layer of ferrocene monosulfonate.

The anion exchange with carbonate anions leads in each case to the same d spacing 7.6 Å, which corresponds to a pure [Zn–Cr–CO$_3$] phase (16). This result confirms that the ferrocene molecules have been removed and that the crystalline network is close to the original one.

The Mössbauer spectra of FMS, FDS, [Zn–Cr–FMS], [Zn–Cr–FDS], [Zn–Cr–FMS/CO$_3$], [Zn–Cr–FDS/CO$_3$], and the reference material [Co–Fe–Cl], recorded at 300 K, are presented in Fig. 3.

Mössbauer spectroscopy is a very interesting technique to study reactions based on ferrocene. The ferrrocene and the ferricinium ion have been intensively studied and their Mössbauer parameters are well defined (17). In ferrocene, iron is in a Fe^{2+} low-spin oxidation state, while it is in a Fe^{3+} high-spin state in the ferricinium ion. They display the same isomer shift (IS) of 0.41 mm/s^{-1} but they can be easily distinguished by very different quadrupole splitting values (QS), which are 2.4 and 0 mm/s^{-1} for ferrocene and ferricinium ion. In FMS and FDS, the values of IS and QS (Table 1) are close to that observed in pure ferrocene, indicating that the iron nucleus is not affected by the presence of sulfonate moieties (Figs. 3a and 3b).

The Mössbauer spectra of [Zn–Cr–FMS] and [Zn–Cr–FDS] (Figs. 3d and 3c) were fitted with quadrupole doublets, and the characteristic singlet of ferricinium ion was never observed. The data show one major (60%) contribution corresponding to the intercalated ferrocene sulfonates (Site I) and a second contribution whose Mössbauer parameters correspond to Fe^{3+} in a high-spin state (Site II). In the case of [Zn–Cr–FDS] a third additional doublet (Site III) of low intensity must be introduced (Fig. 3c). This site appears only after a long acquisition time, and it is characterized by an IS of 1.12 mm/s^{-1} and a QS of 2.49 mm/s^{-1}, corresponding to the classical values observed for Fe^{2+} in a high-spin state. This latter site is likely to originate from a low-spin to high-spin transition and may be a necessary intermediate stage before the ferrocene decomplexation.

The Mössbauer spectra of the [Zn–Cr–FMS/CO$_3$] and [Zn–Cr–FDS/CO$_3$] phases (Figs. 3e and 3f) confirm that iron is still present within these structures, which is in agreement with the elemental analyses. Indeed, the Fe/Cr ratio, given by EDX analyses, which are close to the expected values, 1 in [Zn–Cr–FMS] and 0.5 in [Zn–Cr–FDS], respectively, are not modified in the course of the anion exchange. Spectra can be fitted with two quadrupole doublets whose parameters correspond to Fe^{3+} high spin. Both sites are characterized by very similar isomer shift value ~ 0.36 mm/s^{-1} and slightly different quadrupole splitting (~ 0.6–0.8 mm/s^{-1}, respectively). The values for Site II correspond to those previously observed for the same site in
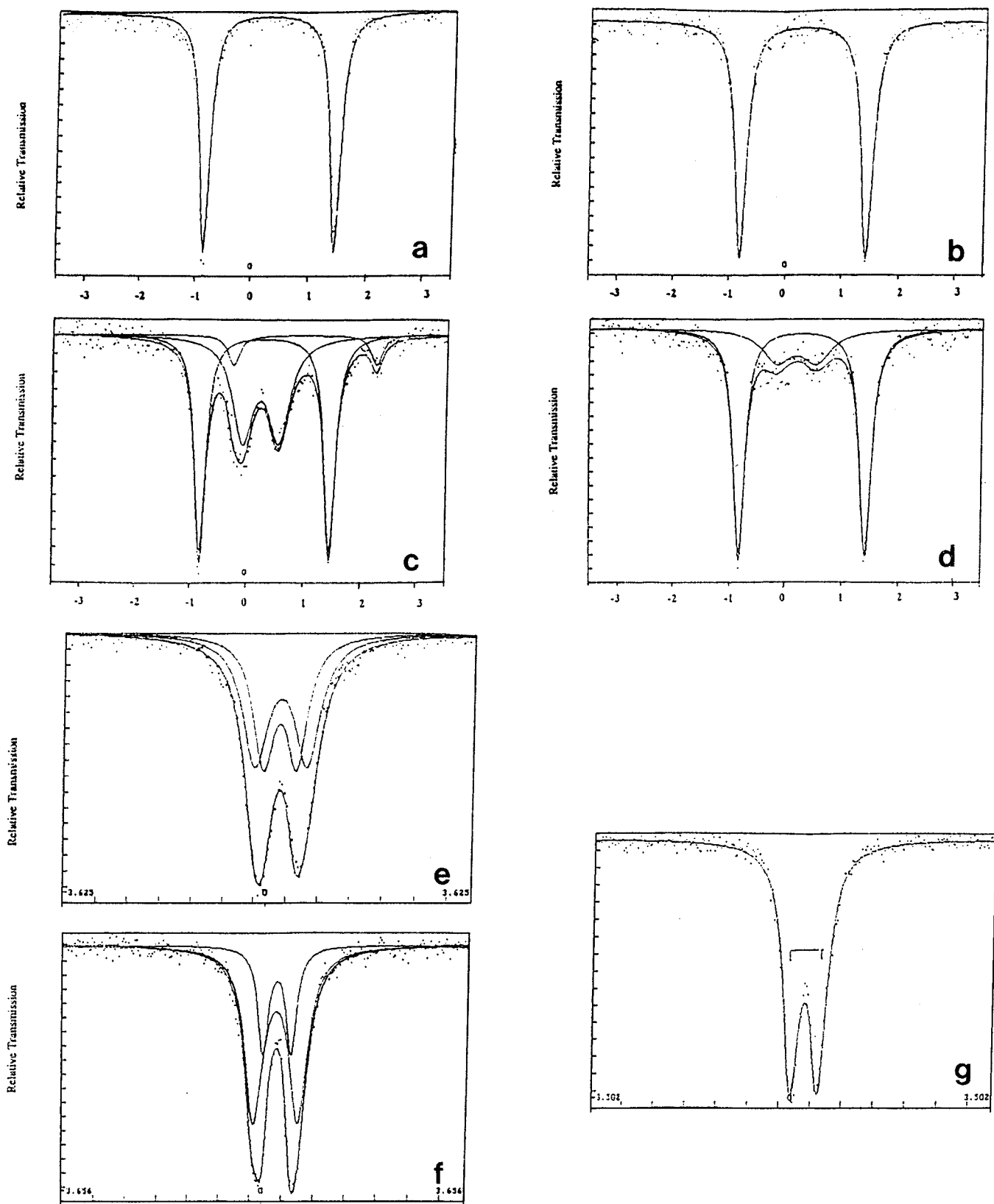
FIG. 3. Mössbauer spectra of (velocity is given in mm/s^{-1}) (a and b) ferrocene disulfonate and monosulfonate, (c and d) [Zn–Cr–FDS] and [Zn–Cr–FMS], (e and f) [Zn–Cr–FDS/CO$_3$] and [Zn–Cr–FMS/CO$_3$], and (g) [Co–Fe–Cl].

TABLE 1
Mössbauer Data (300 K)

Compound	Site	IS (mm/s^{-1})	QS (mm/s^{-1})	W	site %	Assignment
[FDS]		0.41	2.28	0.11	100	Fe^{2+} low spin
[Zn–Cr–FDS]	I	0.44	2.28	0.11	55	FDS
	II	0.36	0.63	0.22	40	Fe^{3+} high spin
	III	1.12	2.49	0.12	5	Fe^{2+} high spin
[Zn–Cr–FcDS/CO$_3$]	I	0.36	0.80	0.19	60	Fe^{3+} high spin
	II	0.37	0.60	0.11	40	"
[Co–Fe–Cl]		0.34	0.47	0.17	100	Fe^{3+} high spin

Note. IS, isomer shift; QS, quadrupole splitting QS = 1/2 eV$_{zz}$D(1 + $\eta^{2/3}$)$^{1/2}$; W, half linewidth at half height (mm/s^{-1}). Fe$_\alpha$ used as a reference. [Co–Fe–Cl] parameters are given as a reference for an iron Fe^{3+} high-spin site in an octahedral environment (6 OH$^-$).

[Zn–Cr–FMS] and [Zn–Cr–FDS]. Furthermore, the percentage of site I corresponds to the amount of ferrocene before anion exchange. Accordingly, there is no more ferrocene sulfonate in the interlayer space but Fe^{3+} cations are present in the structure; no site corresponding to Fe^{2+} cations in a high-spin state is observed.

A cyclic voltammetry study has been performed in aqueous solutions of ferrocene sulfonates to determine the conditions for a possible decomplexation of metallocenes. Linear sweep voltammograms of mono- and disulfonate ferrocenes in aqueous solutions display diffusion-controlled reversible waves which are known to be pH independent in the range 4 to 8 (18). The shift of the formal redox potentials (E°′(FMS) = 0.37 V and E°′(FDS) = 0.60 V) with respect to the unsubstituted ferrocene (E°′(FC) = 0.16 V) is due to the presence of one- or two-electron withdrawing sulfonate groups, indicating an increase in oxidant capacity. Moreover, we have noticed a slow decomposition of FMS and FDS salts in aqueous solution. Indeed, the current peak intensity corresponding to a 5×10^{-4} M FDS aqueous solution decreases slowly with time to finally stabilize after 6 h at a value corresponding to 40–50% of the initial value (Fig. 4). This phenomenon is accompanied by the appearance of an orange precipitate in the flask. The decrease of the current peak intensity seems to be slightly faster when the ferrocene sulfonates are solubilized in an electrolyte solution (0.1 M) (Fig. 3). However, no pH effects have been noticed.

In order to gain further insight into the phenomena and the localization of these iron species after anion exchange, additional measurements have been performed in the case of FDS derivatives.

The behavior of iron species was examined by different physical measurements and we have chosen as reference a well-known double hydroxide of the formula [Co–Fe–Cl], in which iron Fe^{3+} is in an octahedral environment made of six OH$^-$. The Mössbauer spectrum of [Co–Fe–Cl] was fitted with one quadrupole doublet with a characteristic isomer shift and quadrupole splitting of 0.34 and

0.47 mm/s^{-1} (Fig. 3g). These values are very close to the experimental results found in our compounds. Moreover, they are the same as those reported in the literature for a [Co–Fe–CO$_3$] LDH (19) in which the iron site is also octahedral.

The XPS spectrum of the pure ferrocene sulfonate FDS(NH$_4$)$_2$ shows an iron doublet at 707.8 eV (Fe 2p$_{3/2}$) and 717 eV (Fe 2p$_{1/2}$) (Fig. 5a). Similar binding energies are reported in the literature (17). When FDS is intercalated within the LDH interlayer, the XPS spectrum shows two kinds of iron: one corresponding to the FDS with the peak of Fe 2p$_{3/2}$ at 707.8 eV and the other to a peak of 2p$_{3/2}$ at 711.4 eV (Fig. 5b). This peak position is similar to that obtained with the [Co–Fe–Cl] phases (2p$_{3/2}$ at 712 eV) (Fig. 5c). Furthermore, the spectrum obtained with the exchanged phase [Zn–Cr–FDS/CO$_3$] only shows one remaining doublet for which the Fe 2p$_{3/2}$ position is 710 eV (Fig. 5d).

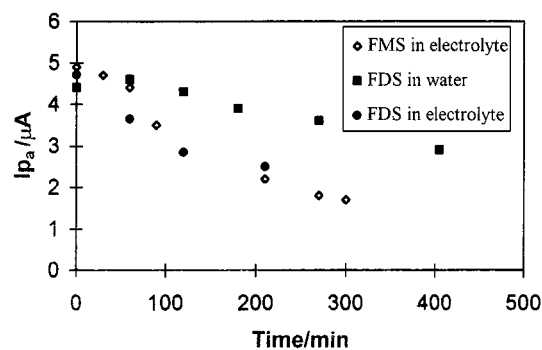A preliminary X-ray absorption study at the Fe–K absorption edge has also been carried out. Figure 6 shows the

FIG. 4. Current peak intensity recorded in linear voltammetry as a function of time (V = 50 mV/s^{-1})/in water: 5×10^{-4} M FDS in water (100 ml), each point corresponds to 10 ml of this solution with 0.1 M LiClO$_4$. In electrolyte: 5×10^{-4} M FMS and 5×10^{-4} M FDS directly solubilized into electrolyte solutions (0.1M KCl and 0.1 M LiClO$_4$, respectively).

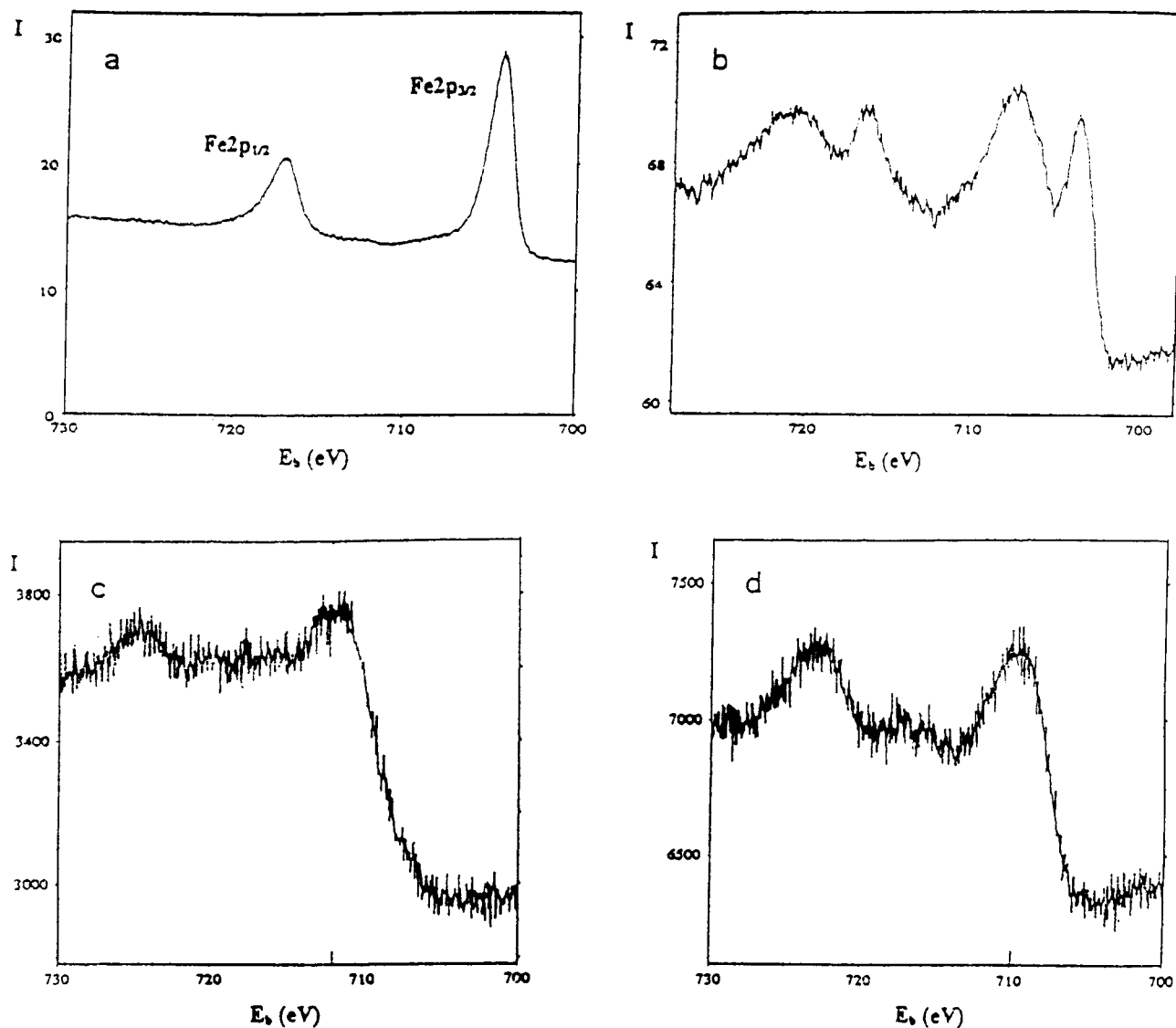**FIG. 5.**   XPS spectra of (a) [FDS], (b) [Zn–Cr–FDS], (c) [Co–Fe–Cl],and (d) [Zn–Cr–FDS/CO$_3$].

Fourier transformed EXAFS spectra of [Zn–Cr–FDS] and [Zn–Cr–FDS/CO$_3$]. These radial distribution functions (RDF) are compared with those of [FDS] salt and [Co–Fe–Cl]. The great similarity in the spectra of [Zn–Cr–FDS] and [FDS] clearly indicates that the environment of Fe ions in these two compounds is the same. Indeed, the (RDF) show only one peak which corresponds to the Fe–C shell; best-fit models were obtained with a coordination number of 10 carbon atoms and Fe–C distances of 2.09 Å. It is noteworthy that no backscattering from elements belonging to the hydroxide sheet is observed in the case of [Zn–Cr–FDS]. On the other hand, the (RDF) of [Zn–Cr–FDS/CO$_3$] resembles closely the (RDF) of [Co–Fe–Cl]. We distinguish essentially two peaks. The first

peaks are similar and correspond to the Fe–O shell. The least- squares fits show distorted octahedral environments with the following Fe–O distances: 2×1.99 to 4×2.07 Å in [Zn–Cr–FDS/CO$_3$] and 4×1.99 to 2×2.14 Å in [Co–Fe–Cl]. The second peaks centered at ca. 2.8 Å without phase correction, are slightly different. They are attributed to the six cations surrounding the Fe ions in the hydroxide sheets. As the compositions are different, one expects different types of interactions, i.e., Fe...Zn/Cr/Fe shell in [Zn–Cr–FDS/CO$_3$] and Fe...Co/Fe in [Co–Fe–Cl]. Though this is a preliminary study, EXAFS results would support the migration of Fe ions from the interlayer space to the hydroxide sheets during anion exchange of FDS by carbonate anions.
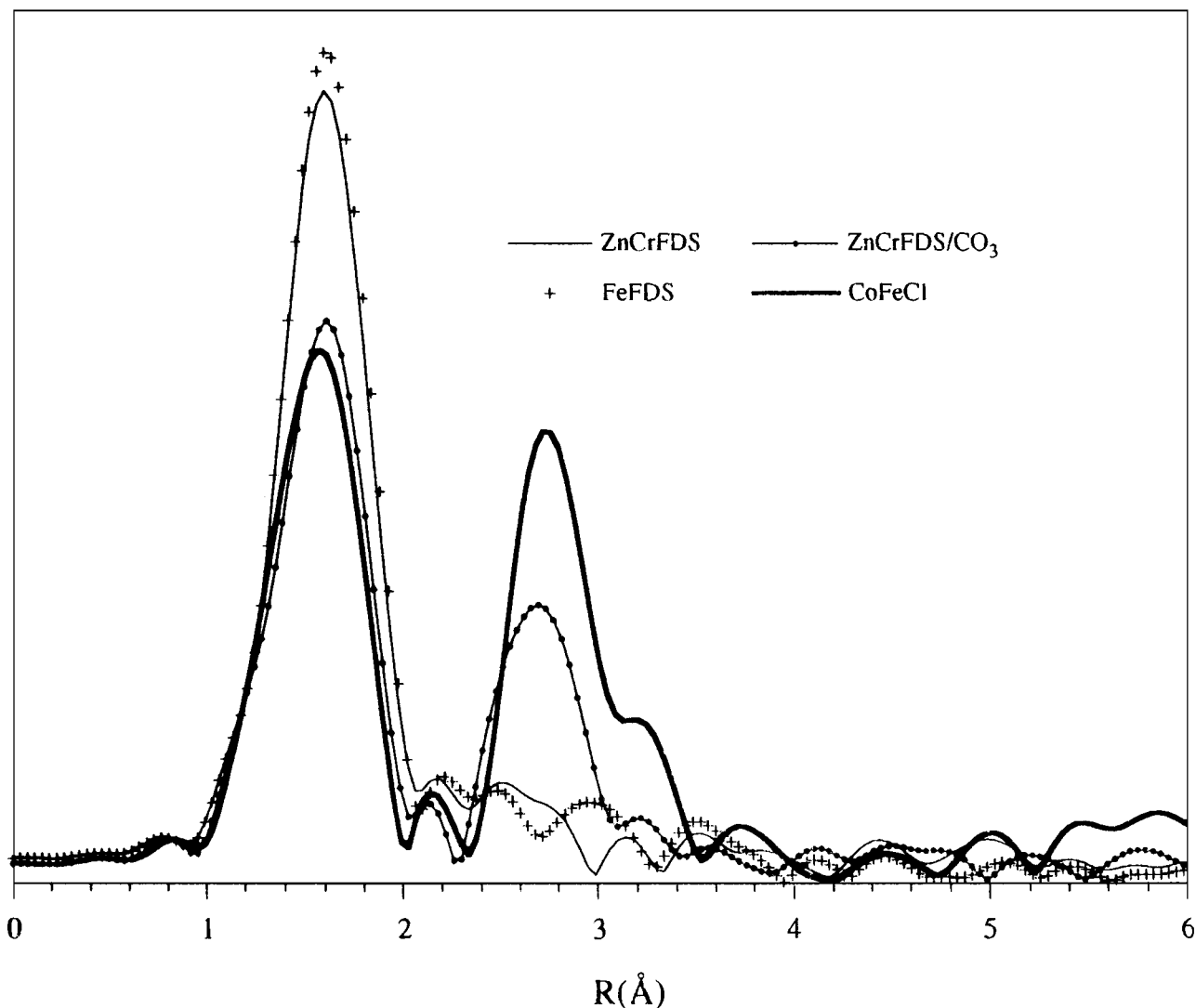
FIG. 6. Fourier transformed spectra of [Zn–Cr–FDS], [Zn–Cr–FDS/CO$_3$], [FDS], and [Co–Fe–Cl].

All these measurements allow us to say that Fe^{3+} ions are in a high-spin state and would very probably localized in the hydroxide layers. If iron atoms were localized in the interlayer space grafted on the hydroxide layers, simulations of PXRD patterns indicate that spectra of [Zn–Cr–Cl] and [Zn–Cr–FDS/CO$_3$] would be different with additional diffraction peaks in the latter compound, and this is not the case.

As a new layer (Zn$_2^{2+}$/Cr^{3+}/Fe^{3+}) replacing the original one (Zn$_2^{2+}$/Cr^{3+}) is obtained, with a different M^{2+}/M^{3+} ratio, interactions between paramagnetic ions may be possible and modifications in magnetic properties are expected. For this reason, susceptibility measurements have been performed between 4 and 300 K.

The starting double hydroxide [Zn–Cr–Cl] obeys the Curie–Weiss law (Fig. 7a) between 4 and 300 K. The effective moment 3.94 μ_B/atom is in agreement with theoretical value expected for a Cr^{3+} (d^3) in a high-spin state without spin orbit contribution (3.87 μ_B/atom). For other samples, chemical formulas are not exactly known and quantitative results must be considered with caution. In ferrocene sulfonates, iron is in a Fe^{2+} (d^6) low-spin state and is consequently diamagnetic. The increase of the Curie constant and the effective magnetic moment (Table 2) is attributed to the presence of Fe^{3+} (d^5) high spin in agreement with the Mössbauer results. The paramagnetic temperature also increases (in absolute value) corresponding to an increase of antiferromagnetic interactions. For this reason, below 50 K the [ZnCrFDS/CO$_3$] compound does not follow the Curie–Weiss law (Fig. 7b).
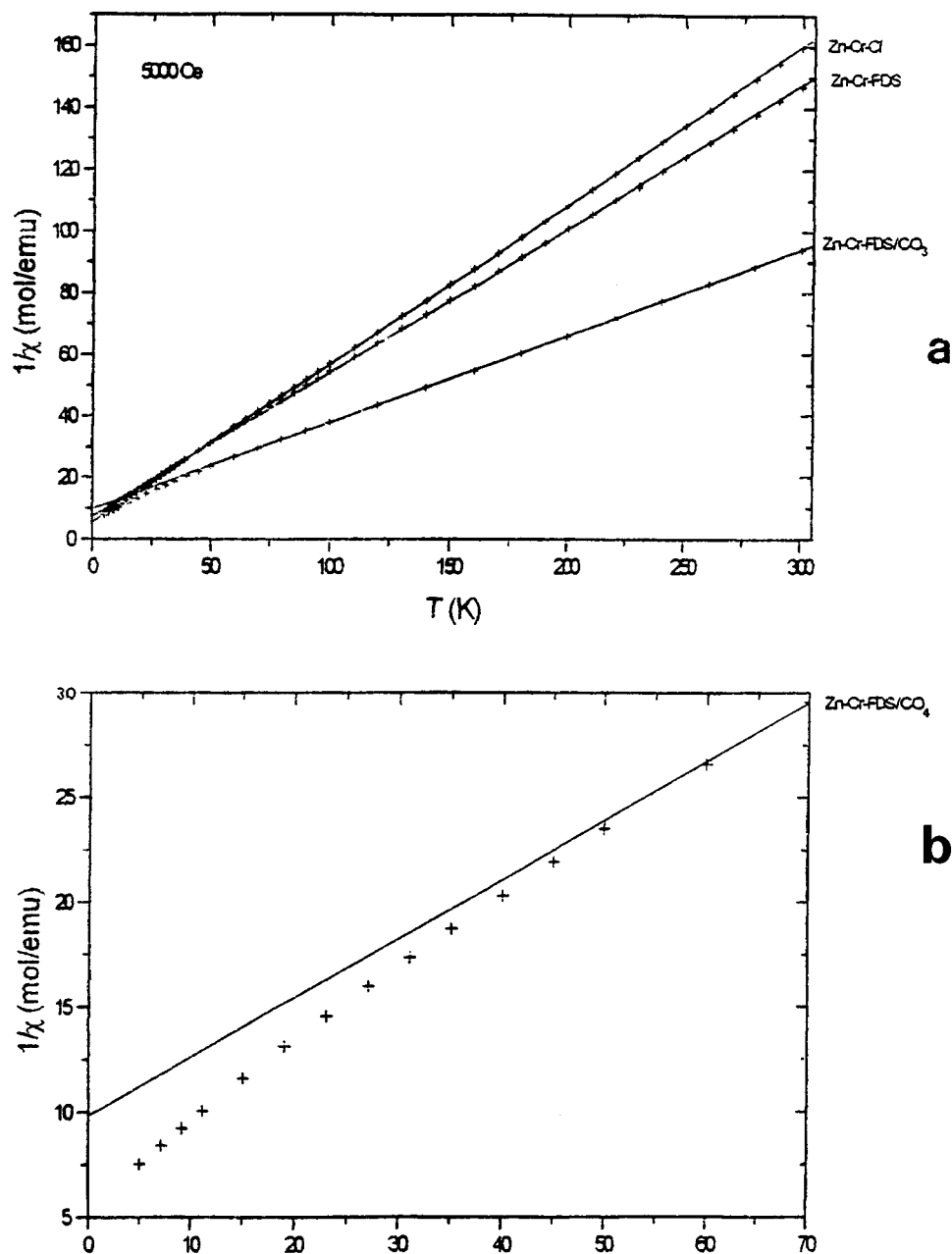
FIG. 7. (a) Temperature dependence of the reciprocal susceptibility curves of [Zn–Cr–Cl], and [Zn–Cr–FDS], and [Zn–Cr–FDS/CO$_3$] in a 5 kOe magnetic field and (b) [Zn–Cr–FDS/CO$_3$]: low temperature range.

CONCLUSION

We have shown the possibility to not only intercalate ferrocene sulfonate salts in some lamellar double hydroxides but also to modify the composition of their layers. The simplest chemical mechanism would be a dissolution–re-building process of the LDH structure with incorporation of iron arising from the simultaneous decomplexation of ferro-cene salts. The resulting chemical reaction can be written

$$[Zn_2Cr(OH)_6][Cl,2H_2O]$$
$$\rightarrow [Zn_2CrFe_{0.5}(OH)_{7.5}][(CO_3)_{0.5},2H_2O].$$
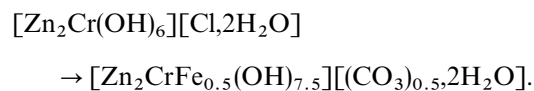
The modification in the distribution of paramagnetic ions in the structure involves a change in magnetic properties.

TABLE 2
Magnetic Susceptibility Results

	[Zn–Cr–Cl]	[Zn–Cr–FDS]	[Zn–Cr–FDS/CO$_3$]
M (g/mol^{-1})	356	493	411
χ_{dia} (-10^{-6} emu/mol^{-1})	151	169	165
C (emu/mol^{-1} K)	1.94	2.14	3.56
θ_p (K)	-10.6	-15.8	-34.9
μ (μ_B/Cr atom)	3.94	4.13	5.33

Note. M, molecular weight; C, Curie constant; θ_p, paramagnetic temperature.

This type of reactions is not limited to [Zn–Cr–Cl] LDH but it is possible in many LDH. Indeed, we have obtained similar results with [Co–Al–Cl] or [Co–Fe–Cl] double hydroxides and an extended study is underway. In the [Co–Fe–Cl] compound, the introduction of iron in a paramagnetic layer leads to fundamental changes in the magnetic properties, particularly the ordering temperature and the nature of interactions. Moreover, this behavior can be modulated versus the quantity of incorporated iron.

REFERENCES

1. A. de Roy, C. Forano, K. El Malki, and J. P. Besse, *in* "Expanded Clays and Other Microporous Solids" (M. L. Occeli and H. E. Robson, Eds), p. 108. Van Nostrand Reinhold, New York, 1992.
2. F. Trifirò and A. Vaccari, *in* "Comprehensive Supramolecular Chemistry" (J. L. Atwood, D. D. MacNicol, J. E. D. Davies, and F. Vogtle, Eds., Vol. 7, p. 251. Pergamon Press, Oxford, 1995.
3. A. Vaccari, *Catalysis Today* **41,** 53 (1998).
4. S. P. Newman and W. Jones, *New J. Chem.* 105 (1998).
5. C. Mousty, S. Therias, C. Forano, and J-P. Besse, *J. Electroanal. Chem.* **374**, 63 (1994).
6. S. Therias and C. Mousty, *Appl. Clay Sci.* **10**, 147 (1995).
7. S. Therias, C. Mousty, C. Forano, and J. P. Besse, *Langmuir* **12,** 4914 (1996).
8. S. Therias, C. Mousty, S. Bonnet, C. Forano, and P. Palvadeau, *Mol. Cryst. Liq. Cryst.* **311,** 195 (1998).
9. S. Therias, B. Lacroix, B. Schöllhorn, C. Mousty, and P. Palvadeau, *J. Electroanal. Chem.* **454**, 91 (1998).
10. G. R. Knox and P. L. Pauson, *J. Chem. Soc.* 692 (1958).
11. A. Michalowicz, "Thèse d' état," Paris, 1990.
12. P. Seiler and J. D. Dunitz, *Acta Crystallogr., Sect. B* **35,** 1068 (1979).
13. P. Palvadeau, L. Coic, J. Rouxel, F. Menil, and L. Fournes, *Mater. Res. Bull.* **16,** 1055 (1981).
14. H. V. Wong, J. S. O. Evans, S. Barlow, and D. O'Hare, *J. Chem. Soc. Chem. Comm.* 1589 (1993).
15. H. Takaya, T. Hashimoto, M. Karasu, T. Izumi, and K. Chiba, *Chem. Lett.* 2113 (1993).
16. A. de Roy, J. P. Besse, and P. Boudot, *Mater. Res. Bull.* **33,** 5363 (1994).
17. H. Eckert, *in* "Mossbauer Spectroscopy Applied to Inorganic Chemistry" (G. Long, Ed.), Vol. 2, p. 188. Plenum Press, New York, 1987.
18. H. C. B. Hansen, C. B. Buck, and R. M. Taylor, *J. Solid State Chem.* **113,** 21 (1995).
19. D. J. Walton, C. E. Hall, and A. Chyla, *Synth. Metals* **45,** 363 (1991).